

---

# THEORY AND SIMULATIONS OF NONLINEAR SBS IN MULTISPECIES PLASMAS

*S. C. Wilks      D. E. Hinkel      B. MacGowan*  
*W. L. Kruer      K. Estabrook      D. S. Montgomery*  
*J. Denavit      D. Kalantar      E. A. Williams*  
*A. B. Langdon*

---

## Introduction

Stimulated Brillouin scattering (SBS) is an instability in which intense laser light incident on a target can decay into a scattered light wave and an ion sound wave. The process requires frequency and wavenumber matching (i.e.,  $\omega_o = \omega_{sc} + \omega_i$  and  $k_o = k_{sc} + k_i$ ), which corresponds to energy and momentum conservation. Here,  $\omega_o$  ( $\omega_{sc}$ ) is the frequency of the incident (scattered) light wave and  $\omega_i$  is the frequency of a sound wave in the plasma, and  $k_o$ ,  $k_{sc}$ , and  $k_i$  are the corresponding wavenumbers. It is important to understand and control this instability to optimize energy deposition in inertial fusion targets.

SBS arises in two distinct places within a gas-filled hohlraum target. First, the gas in the hohlraum is ionized within the first couple of pico-seconds of the laser pulse, so the rest of the nanosecond pulse sees a plasma ( $\sim 0.1 n_c$ ) as it propagates toward the wall of the hohlraum. At later times, the ablation from the Au wall of the hohlraum becomes underdense and allows for the generation of SBS. It has been proposed that mixed species plasma, both in the gas and the wall of the hohlraum, can minimize the energy transferred to the ion waves and the reflected light, maximizing the amount of laser energy available for conversion to x-rays.

This article presents detailed particle-in-cell simulation studies of SBS in underdense plasmas composed of two and three distinct ion species.<sup>1</sup> Collisionless nonlinear saturation mechanisms are well modeled. For the parameters discussed here, these mechanisms depend critically on plasma composition. The effect of a self-consistently evolved non-Maxwellian distribution for the light ions on the ion-wave amplitude can be observed in detail. Mixtures of H and He are used to illustrate the physics of the situation. Various mixtures of “heavy” ions (carbon) and “light” ions (deuterium–

hydrogen) are also studied in these simulations. The reflectivity and ion-wave amplitudes due to the SBS instability show many of the trends seen in experiments with these gases.

Alexeff, Jones, and Montgomery<sup>2</sup> investigated the effects of adding a light-ion species to a plasma composed primarily of a heavier, more abundant ion species. Their experiments show that the damping of the ion wave increases as significant amounts of the lighter species are introduced. This result agrees with a linear ion Landau damping model by Fried and Gould.<sup>3</sup> Clayton et al.<sup>4</sup> used a CO<sub>2</sub> laser to confirm many of the predictions in the linear regime. Although additional research has been done,<sup>5,6</sup> the nonlinear aspects of adding a light species to a plasma have been neglected. Some insight into this state is important since recent experiments<sup>7–9</sup> with intense laser light ( $I \approx 3 \times 10^{15}$  W/cm<sup>2</sup>, wavelength 0.351  $\mu$ m, pulse duration  $\tau_p \approx 1$  ns) and relatively high plasma density  $\sim 0.1 n_c$  (where  $n_c$  is the critical density) are thought to operate in a nonlinearly saturated state.

## Computational Technique

We use the electron-fluid, particle-ion code EPIC to study various kinetic nonlinearities for saturation of the ion wave associated with SBS. Kinetic nonlinearities, such as particle trapping and extreme modification of the velocity distribution function arise when individual particle motion becomes important. Bulk “fluid” motion does not resolve individual particle velocities and cannot include single particle effects. An interesting comparison with linear theory is observed; however, there are significant differences. We find that particle trapping can substantially lower the ion-wave amplitude when a light-ion species is present in a predominantly heavy-ion plasma. These results agree with simple

nonlinear theories. Even in the nonlinear state, trace amounts of light ions can substantially reduce the reflectivity arising from SBS in a heavy-ion plasma.

A brief explanation of the simulation code illustrates the physics accessible in this study. EPIC resolves the electromagnetic (EM) wave associated with the laser light, both spatially and temporally, using the Langdon–Dawson advection scheme.<sup>10</sup> In one dimension, the light can be broken up into right- ( $E_+$ ) and left-going ( $E_-$ ) waves that advect exactly at the speed of light  $c$ :

$$\left(\frac{\partial}{\partial t} \pm c \frac{\partial}{\partial x}\right) E_{\pm} = -\frac{1}{2} J_y = \frac{1}{2} n_e e v_y, \quad (1)$$

where  $J_y$  is the transverse current,  $e$  is the electron charge, and  $n_e$  is the electron plasma density. In the presence of a plasma, the transverse velocity  $v_y$  of the electrons serves as the source for the EM waves. The ponderomotive potential  $U_p = 1/2 m v_y^2$ , where  $m$  is the electron mass, is saved every time step. This is an essential component of the feedback loop in the SBS instability because it couples the reflected light wave to the ion-density fluctuations, which then grow exponentially, according to linear theory. The ion-density fluctuation has a wavenumber  $2k_0$  and frequency  $\omega_{ia} = 2k_0 c_s$ , where  $c_s = (ZT_e/M_i)^{1/2}$  is the ion sound speed,  $T_e$  is the electron temperature,  $Z$  is the ion charge state, and  $M_i$  is the ion mass. Since the ions move slowly on the time scale of the laser light, they need not be moved every time step. Instead, they are moved every 200th time step or so, by an amount determined by a time average of  $U_p$  over this time interval. EPIC handles the ions as particles, and the force on these ions is that due to the electrostatic field obtained from the electron momentum equation [(Eq. (2))], where the electrons are taken to be a massless fluid. Neglecting electron inertia is a good approximation, in that  $m$  is much less than  $M_i$ , so that the electrons can respond to bulk ion motion instantaneously on the ion time scale. Hence, the electrostatic field felt by the ions is

$$E_x = -\frac{1}{e} \left[ \frac{\partial \langle U_p \rangle}{\partial x} - \frac{1}{n_e} \frac{\partial (n_e) T_e}{\partial x} \right], \quad (2)$$

where  $\langle U_p \rangle$  represents the time-averaged value of  $U_p$ . Once this electrostatic field is known, the ions are then moved on the grid according to the equation

$$\frac{dv_i}{dt_i} = \frac{Z_i}{M_i} E_x,$$

where

$$\frac{dx_i}{dt_i} = v_i. \quad (3)$$

Here, the  $dt_i$  denotes the ion time scale. Once the ions are at the new positions, the ion density  $n_i$  is computed. This is done for all ion species, usually two or three species with different masses  $M_j = A_j M_p$  and charge states  $Z_j$ . Here  $M_p$  is the mass of the proton and  $A_j$  ( $Z_j$ ) is the atomic number (charge state) of the  $j$ th ion. Finally, a new electron density is found by summing the ion density contributions over all species at each grid point, and setting  $n_e$  equal to this total ion density. The EM waves are then advected for another 200 time steps, and the process is repeated. (Reference 1 gives further details of the computational model and approximations.)

## Experimental Motivation

The motivation for these simulations is a set of recent experimental results obtained on the Nova laser using “gas bags”<sup>7</sup> and gas-filled hohlraums.<sup>8,9,11</sup> Briefly, these experiments measured the reflectivity due to SBS from a number of large-scalelength ( $\sim 1$  mm), low-density ( $\sim 0.1 n_c$ ) plasmas composed of a variety of gases, such as  $C_5H_{12}$ ,  $C_5D_{12}$ , and  $CO_2$ . The simulations presented here attempt to describe some of the trends in the experimental data. For all simulations,  $T_e = 3$  keV, and the ratio of  $T_e$  to the initial  $T_i$  is always in the range  $3 \leq T_e/T_i \leq 10$ . The laser wavelength is  $\lambda_0 = 0.351 \mu m$ , and the intensity is  $I = 2.7 \times 10^{15} W/cm^2$ , as in the experiment. The density is typically either  $0.1 n_c$  or  $0.25 n_c$ , and the system length is usually  $L_x = 75, 150$ , or  $330\lambda_0$ . Roughly 1 million particles per ion species are used for the longer systems. Occasionally, the noise was increased to large levels to accelerate the onset of a nonlinear, quasi-stationary state. The reflected wave grows from a noise level  $I_{noise}$ , which is set by scattering of the incident wave from ion-density fluctuations. In these simulations,  $I_{noise}/I_0$  is of the order 1%, but can be as low as 0.01%.

A few caveats concerning comparison of these simulations with experimental results are as follows: (1) The ions are constrained to move in one dimension in the simulation. Various two- and three-dimensional results, such as finite speckle width, filamentation, ion transport, and scattering of the ion waves in angle, are expected to reduce the reflectivity observed in the experiments. (2) The system is chosen to be roughly one speckle length long (for an  $f/4$  lens), as opposed to the much longer system present in the experiments ( $\sim 1$  mm). (3) The simulations are only run for 10–20 ps, as opposed to a nanosecond for the experiment. However, linear gain calculations of this laser–plasma interaction consistently predict excessive gains, indicating that some nonlinear processes are at work to limit the reflectivities. Despite these differences, we hope to gain insight into some of the nonlinear saturation and damping mechanisms that may be playing a role in current experiments. We concentrate on the trends seen

in the simulations and experiments for various parameters and not on the absolute values of the reflectivity.

## Theory

Linear theory predicts that trace amounts of light ions substantially increase the ion Landau damping of the ion wave. There are several reasons for this effect. (1) If we assume that the  $T_i$  are the same, the higher thermal velocity for the light-ion species leads to more ions in resonance with the wave. (2) The phase velocity is a function of the plasma composition. To illustrate this, consider the linearized ion continuity and momentum equations for the two fluids:

$$\frac{\partial n_{i1}}{\partial t} + n_{i10} \frac{\partial u_{i1}}{\partial x} = 0, \quad (4)$$

$$\frac{\partial n_{i2}}{\partial t} + n_{i20} \frac{\partial u_{i2}}{\partial x} = 0$$

and

$$\frac{\partial u_{i1}}{\partial t} = -\frac{Z_1}{M_1} k T_e \frac{1}{n_{e0}} \frac{\partial n_e}{\partial x}, \quad (5)$$

$$\frac{\partial u_{i2}}{\partial t} = -\frac{Z_2}{M_2} k T_e \frac{1}{n_{e0}} \frac{\partial n_e}{\partial x}.$$

By combining Eqs. (4) and (5) into one equation for the ion wave, an effective phase velocity  $v_p$  for the ion wave is found to be

$$v_p^2 = \frac{n_{i10} \frac{Z_1^2 k T_e}{M_1} + n_{i20} \frac{Z_2^2 k T_e}{M_2}}{Z_1 n_{i10} + Z_2 n_{i20}}. \quad (6)$$

Figure 1 plots this phase velocity for C and H at  $T_e = 3$  keV, as a function of the fraction of H in the gas mixture. The limit in which only C ions are present smoothly connects to the case for only H present. Note that the phase velocity falls rapidly from the pure H case, essentially because the phase velocity is determined by the heavy species when the fraction of H is roughly 50%.

The physics can be clarified by considering the velocity distribution function  $f(v)$  of two ion populations with different atomic numbers and charge states. Consider first pure He, as shown in Fig. 2. Notice the small slope and the small number of particles at the phase velocity of the ion wave  $v_p$  ( $n_H = 0$ )  $\equiv c_{sHe}$  available to damp the SBS-generated ion wave. Now consider pure H at the same  $T_i$ . The slope at  $v_p$  ( $n_{He} = 0$ )  $\equiv c_{sH}$  is somewhat greater than for pure He, and there are more particles at

this phase velocity. Finally, consider a mixture of 20% H and 80% He, where  $v_p$  is now given in accordance with Eq. (6) and is approximately equal to  $c_{sHe}$  (see Fig. 2). In this case, a large number of H ions can now damp the ion wave even more efficiently than in pure H, because the phase velocity has moved farther into the bulk of the distribution function. Thus, linear theory predicts that the damping for the mixture will actually be greater than for H alone (and thus give the lowest reflectivity), and that pure He will have the least damping (and the highest reflectivity). Simulations bear out this prediction. For simulations with parameters similar to those discussed earlier, pure He gives a reflectivity  $R \approx 30\%$ , pure H gives  $R \approx 10\%$ , and the 20% H and 80% He give  $R \approx 5\%$ .

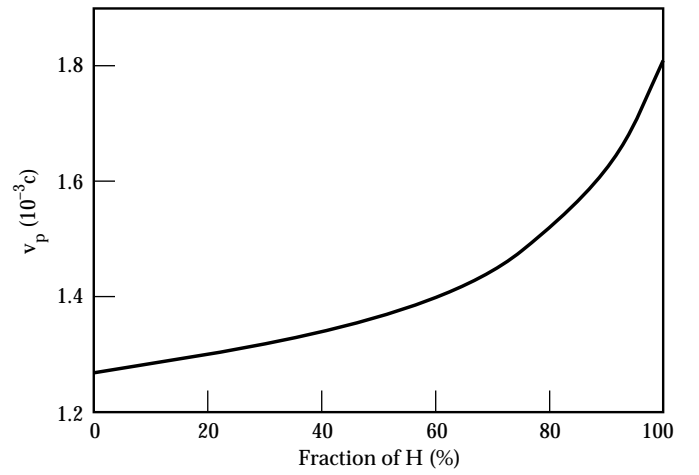


FIGURE 1. Acoustic wave phase velocity vs fraction of H present in a CH plasma. (50-00-0495-1065pb02)

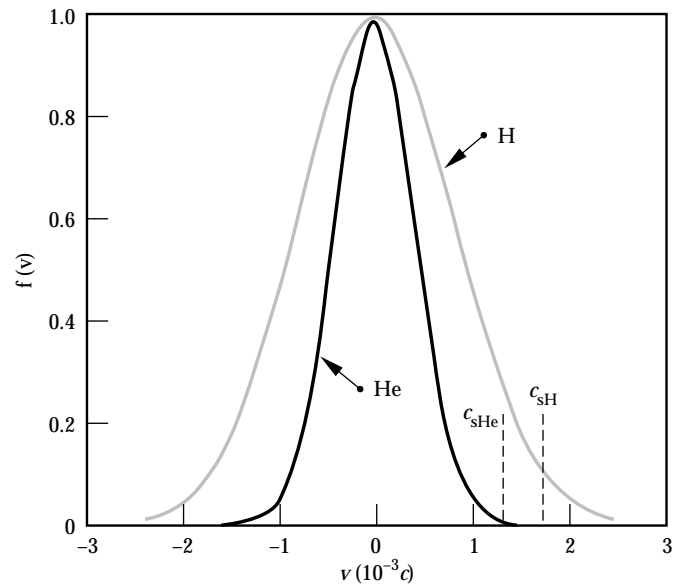


FIGURE 2. Ion distribution functions for a pure He plasma and a pure H plasma, for  $T_e = 3$  keV and equal  $T_e/T_i$ . (50-01-0695-1418pb02)

## Particle Trapping

We have discussed the effect of plasma composition on linear damping of the ion acoustic wave. However, the simulations show that nonlinear effects can be important when the reflectivity is significant. Let us now examine the simplest nonlinear effect, which is ion trapping. When the ion trapping velocity is equal to the phase velocity of the ion wave, the amplitude of the density perturbation associated with the ion wave will saturate. For one species, this limiting amplitude (neglecting temperature effects) is the well-known result  $\delta n/n = 1/2$ ,<sup>1</sup> where  $\delta n$  is the low-frequency fluctuation in  $n_e$  associated with the ion wave. For two species, assuming cold ions ( $T_i \approx 0$ ), the limiting amplitude of the density perturbation is found to be  $\delta n/n = 0.25$  when the light species is H. This factor-of-2 difference arises from the fact that the H ions are the particles being trapped in a wave with a phase velocity determined by the heavy fluid. The assumption here is that there is only a small amount of the light ions in the mixture. However, when  $T_i$  effects are included, the limiting amplitude is considerably reduced to

$$\left(\frac{\delta n}{n}\right)_{tr} \approx \frac{1}{2T_e} \left(\frac{M_1}{Z_1}\right) \left(v_p - \sqrt{\frac{3T_i}{M_1}}\right)^2, \quad (7)$$

where the phase velocity is found from

$$v_p^4 + v_p^2 (\omega_{pH}^2 \lambda_{De}^2 + \omega_{pC}^2 \lambda_{De}^2 + 3v_{pH}^2) + 3v_{pH}^2 \omega_{pC}^2 \lambda_{De}^2 = 0. \quad (8)$$

Here,  $\lambda_{De}$  is the Debye length,  $\omega_{pH}$  is the plasma frequency of the light-ion species (H), and  $\omega_{pC}$  is the plasma frequency of the heavy ions (C). For a temperature ratio  $T_e/T_i = 10$ , Eq. (7) predicts  $(\delta n/n)_{tr} \approx 5\%$ .

The EPIC simulations show the nonlinear state to be very rich. For example, for the case of  $C_5H_{12}$ , the H ion distribution function near  $v_p$  initially flattens due to ion trapping, as discussed. However, a number of effects follow. (1) As the ion waves grow and ions are pulled out of the initially Maxwellian distribution, a severe modification of the distribution function near  $v_p$  occurs [see Fig. 3(a)]. When a “bump” is present in a distribution function, the distribution function is unstable to ion sound waves near  $v_p$ . The ions have a tendency to relax back to a more stable distribution function, sometimes called a “quasilinear plateau.” This is essentially a flat slope near  $v_p$ . However, it is found that before the distribution function reaches this state, it over-shoots the plateau and re-develops a slope near  $v_p$  [see Fig. 3(b)]. Thus, the distribution function will “oscillate” about

this point. The distribution function inside the trapping width oscillates at the bounce frequency  $\omega_B$ , as predicted by O’Neil.<sup>12</sup> As the distribution function evolves, there is a nonlinear frequency shift due to modifications that the trapped ions make on the ion wave, which reduce  $v_p$ . This allows the instability to access “fresh” slope on the distribution function. An additional effect that works to widen the plateau region is the transport of the faster,

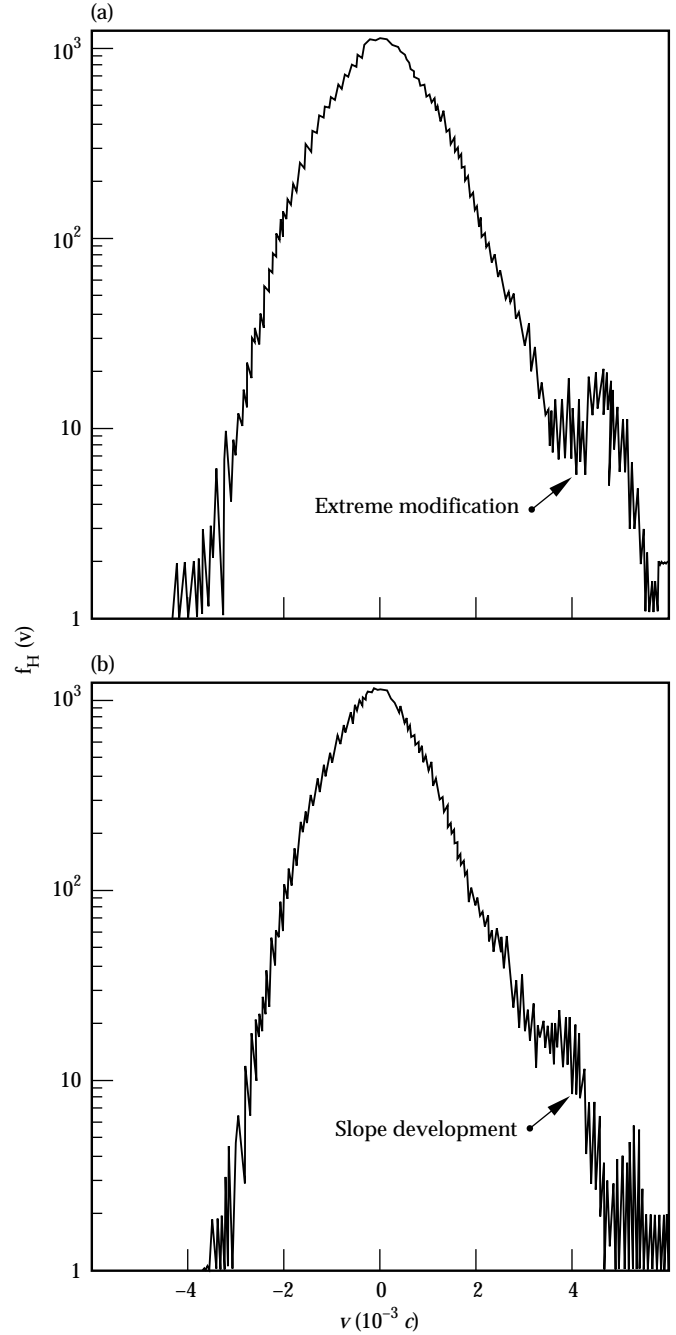


FIGURE 3. Ion distribution for the H component in a  $C_5H_{12}$  plasma showing (a) an extreme nonlinear modification early in time and (b) subsequent development of slope later in time near the phase velocity of the ion wave associated with SBS. (50-00-0495-1066pb02)

heated ions. This allows for a redevelopment of the slope, permitting additional damping.

We now compare EPIC simulations with experimental results in which the fraction of light ions (H) in the gas mixture varies, and the reflectivity is measured for two gas mixtures,  $\text{CO}_2 + \text{C}_3\text{H}_8$  and  $\text{C}_5\text{H}_{12} + \text{C}_3\text{H}_8$ . By increasing the amount of propane in each mixture, the reflectivity as a function of H present decreased strongly in the gas-bag experiments.<sup>7-9</sup> This agrees with experiments in which this phenomenon was observed using a  $\text{CO}_2$  laser.<sup>4</sup> The EPIC simulation results shown in Fig. 4 exhibit a similar trend. In the simulations, the gas starts out as pure C, and H is continuously added (eliminating C to keep the same plasma density) until the gas is pure H. Clearly, varying the plasma composition by adding H is an important technique for reducing the level of SBS.

## SBS in Gas-Filled Hohlräume

Current hohlraums are filled with a low-density gas, which slows the inward motion of the Au walls and improves the time-dependent symmetry of the x-ray flux on the capsule. As discussed, SBS in the low-density gas is reduced by the presence of H. (An H-He mixture is planned for ignition hohlraums.) However, it is necessary to avoid significant SBS from the low-density Au near the walls, where the ion wave is weakly damped. Indeed, this SBS could be a seed that is further amplified in the low-density gas.<sup>8</sup>

A series of simulations has been conducted to understand the Au wall-gas interface. Figure 5 shows the variation of plasma density along the direction of the laser beam when the reflectivity has saturated ( $\approx 20$  ps). In this simulation, four-fifths of the plasma is a  $\text{C}_5\text{H}_{12}$  gas at  $0.1 n_c$ , and the last fifth of the plasma is Au at  $0.12 n_c$ . Initial values are  $T_e = 3.0$  keV,  $T_e/T_i = 2.0$  for Au,  $T_e/T_i = 5$  for H, and  $T_e/T_i = 5$  for C. The laser  $I = 2.7 \times 10^{15} \text{ W/cm}^2$ . As shown in Fig. 5, a substantial ion wave develops in the Au. However, because of the H in the gas, the ion density perturbation in the  $\text{C}_5\text{H}_{12}$  is quite low. In this simulation,  $R \approx 6.0\%$ . In a similar simulation using identical parameters but without the Au wall,  $R \approx 2.0\%$ . Clearly, the presence of low-density Au near the hohlraum wall can significantly affect the reflectivity.

One proposed solution is to use Be-doped Au for the hohlraum wall.<sup>13</sup> However, there is an additional complication when one attempts to model Au-Be; namely, collisions between the Au and Be ions. Simply, estimates of collision times are roughly equal to the time it takes to flatten the slope (see the discussion associated with Fig. 3). This introduces yet another enhanced damping mechanism—collisional damping. This is due to the fact that collisions can

“keep the slope,” thus increasing the range of validity of linear theory since the distribution function can remain more or less Maxwellian. Therefore, further study of the Au-Be wall requires that collisions be included in the simulation code. Preliminary studies with a collisional code<sup>14</sup> have shown that the addition of Be does in fact reduce SBS in the Au-wall blow-off. This is in agreement with recent experiments on the Nova laser.<sup>14,15</sup>

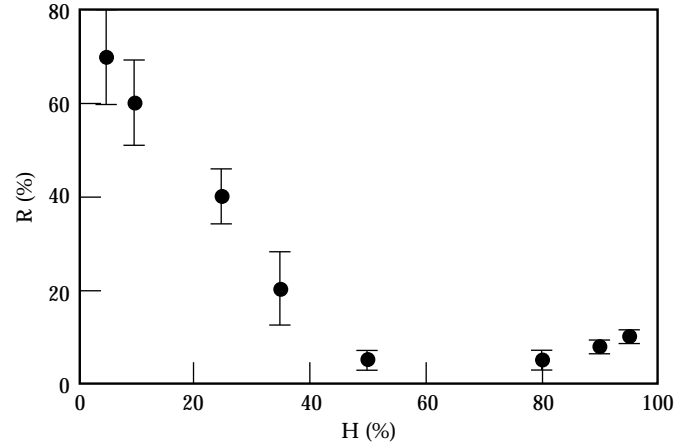


FIGURE 4. Simulation results of reflectivity vs percentage of H present in the plasma. Clearly, the inclusion of small quantities of H can significantly reduce the SBS reflectivity in the nonlinear state. (50-01-0695-1421pb01)

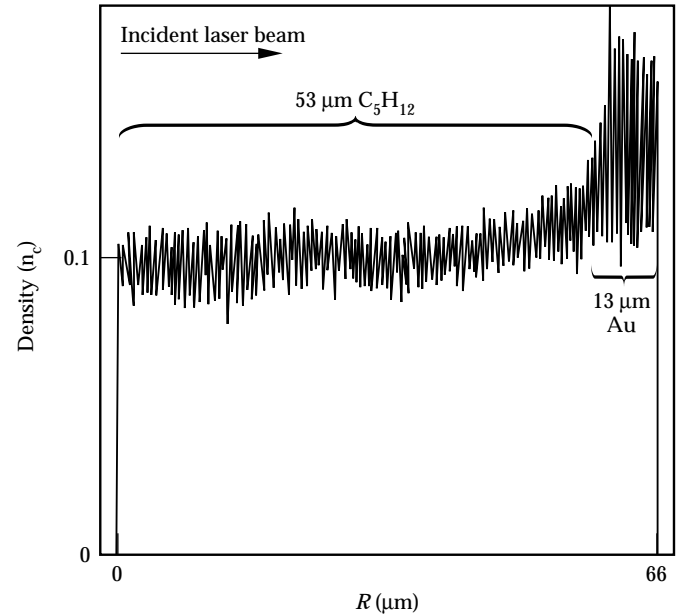


FIGURE 5. Density profile of an EPIC simulation modeling the interface between a low-density gas and the Au wall blow-off of a hohlraum. Note that the Au is initially in the last one-fifth of the plasma. (50-01-0695-1422pb01)

## Summary

This article presents a detailed study of nonlinear processes associated with SBS in a multi-ion-species plasma. We theoretically estimate and compare a number of these nonlinear effects with EPIC kinetic multi-ion-species simulations results and with recent experiments. EPIC results for reflectivities are consistent with the trends observed in experiments. We provide a physical argument for the linear damping in a multispecies plasma, obtaining a simple physical picture of the role light ions play in the damping of the ion waves associated with SBS. We also address the modifications to ion trapping, an inherently nonlinear process, when two species are present and find that the addition of a light species could greatly decrease the amplitude of the ion wave where trapping will occur. These simulations show that distortion in the ion distribution functions can play an important role in determining the amount of reflectivity due to SBS observed in recent experiments. We illustrate a solution to the possible problem of significant SBS due to the low-density Au in gas-filled hohlraums.

## Notes and References

1. S. C. Wilks, W. L. Kruer, D. E. Hinkel, E. A. Williams, et al., *Phys. Rev. Lett.* **74**, 5048 (1995).
2. I. Alexeff, W. D. Jones, and D. Montgomery, *Phys. Rev. Lett.* **19**, 422 (1967).
3. B. Fried and R. W. Gould, *Phys. Fluids* **4**, 139 (1961).
4. C. E. Clayton, C. Joshi, A. Yasuda, and F. F. Chen, *Phys. Fluids* **24**, 2312 (1981).
5. E. A. Williams, et al., *Phys. Plasmas* **2**, 129 (1995).
6. H. X. Vu, et al., *Phys. Plasmas* **1**, 3542 (1994).
7. B. MacGowan, et al., *Bull. Am. Phys. Soc.* **39**, 1662 (1994).
8. J. Fernandez, et al., *Bull. Am. Phys. Soc.* **39**, 1663 (1994).
9. R. Turner, et al., *Bull. Am. Phys. Soc.* **39**, 1662 (1994).
10. A. B. Langdon and J. M. Dawson, *Proc. First Conf. Num. Sim. Plasmas*, College of William and Mary, Williamsburg, VA. 39–40, 19–21 (1967).
11. G. F. Stone, C. J. Rivers, M. R. Spragge, and R. J. Wallace, *ICF Quarterly Report* **5**(3), 151, Lawrence Livermore National Laboratory, Livermore, CA, UCRL-LR-105821-95-3 (1995).
12. T. M. O'Neil, *Phys. Fluids* **8**, 2255 (1965).
13. K. Estabrook, et al., *Bull. Amer. Phys. Soc.* **40** (1995).
14. P. Rambo, W. L. Kruer, and S. C. Wilks, *Bull. Amer. Phys. Soc.* **40** (1995).
15. R. Kirkwood, et al., *Bull. Amer. Phys. Soc.* **40** (1995).